Helical edge and surface states in HgTe quantum wells and bulk insulators

Xi Dai,[1,2] Taylor L. Hughes,[3] Xiao-Liang Qi,[3] Zhong Fang,[1] and Shou-Cheng Zhang[3]
[1]*Beijing National Laboratory for Condensed Matter Physics, Institute of Physics, Chinese Academy of Sciences, Beijing 100080, People's Republic of China*
[2]*Department of Physics, University of Hong Kong, Pokfulam Road, Hong Kong*
[3]*Department of Physics, McCullough Building, Stanford University, Stanford, California 94305-4045, USA*
(Received 10 May 2007; revised manuscript received 27 December 2007; published 14 March 2008)

The quantum spin Hall (QSH) effect is the property of a new state of matter which preserves time reversal, has an energy gap in the bulk, but has topologically robust gapless states at the edge. Recently, the QSH state has been theoretically predicted and experimentally observed in HgTe quantum wells [B. A. Bernevig *et al.*, Science **34**, 1757 (2006); M. Konig *et al.*, *ibid.* **318**, 766 (2007)]. In this work, we start from realistic tight-binding models and demonstrate the existence of the helical edge states in HgTe quantum wells and calculate their physical properties. We also show that three-dimensional HgTe is a topological insulator under uniaxial strain and show that the surface states are described by single-component massless relativistic Dirac fermions in 2+1 dimensions. Experimental predictions are made based on the quantitative results obtained from realistic calculations.

DOI: 10.1103/PhysRevB.77.125319 PACS number(s): 71.55.Gs, 73.20.At, 85.75.−d

I. INTRODUCTION

Conventional insulators have a gap for all charge excitations and their physical properties are not sensitive to changes in the boundary conditions. Recently, a new class of quantum spin Hall (QSH) in two dimensions, or *topological* in three dimensions, insulators has been proposed theoretically and observed experimentally.[1–6] The QSH insulators are invariant under time reversal, have a charge excitation gap in the bulk, but have topologically protected gapless edge states that lie in the bulk insulating gap.[3,7,8] This type of insulator is typically realized in spin-orbit coupled systems, and the corresponding edge states have a distinct helical property: states with opposite spins counterpropagate at the sample edge. The helical edge states are responsible for the intrinsic spin Hall effect in the insulating state.[9–12] The edge states come in Kramers doublets, and time-reversal symmetry (TRS) ensures the crossing of their energy levels at special points in the Brillouin zone (BZ). Because of this level crossing, the spectrum of a QSH insulator cannot be adiabatically deformed into that of a topologically trivial insulator without helical edge states; therefore, in this precise sense, the QSH insulators represent a topologically distinct new state of matter. In three dimensions, the class of strong topological insulators has a similar distinction[5,13] and is the natural generalization of the QSH insulator.

The study of the QSH effect in quasi-two-dimensional (2D) HgTe/CdTe quantum wells carried out in Ref. 1 is based on a simplified model obtained by the $\mathbf{k}\cdot\mathbf{P}$ perturbation theory and the envelope function approximation. The conclusion of a topological quantum phase transition is reached based on a Dirac-type subband level crossing at the Γ point. However, as is shown in the present work, such a level crossing is not generic and is avoided in the real system due to the bulk inversion asymmetry (BIA) of the zinc-blende lattice. Consequently, a more realistic study is necessary to obtain a better understanding of the QSH phase and the topological phase transition. In this paper, we study the subband structure and edge state properties of HgTe/CdTe quantum wells using a realistic tight-binding (TB) model. The level crossing avoided at the Γ point is recovered at several finite wave vectors. In other words, the phase transition between two different insulating regions remains robust despite inversion symmetry breaking. Furthermore, the topological nature of the QSH regime is demonstrated explicitly by studying the properties of the helical edge states in an open boundary system. We also apply the same realistic TB calculations to uniaxial strained three-dimensional (3D) HgTe and obtain the topologically nontrivial surface states. Thus, strained, bulk HgTe is demonstrated to be a strong topological insulator, which is consistent with theoretical analysis based on the Z_2 topological invariants.[13]

II. TIGHT-BINDING MODEL AND GREEN'S FUNCTION METHOD

The CdTe and HgTe materials have the same zinc-blende lattice structure and are well described by the same type of tight-binding Hamiltonian, albeit with different parameters. This Hamiltonian includes two *s*-type orbitals and three *p*-type orbitals on each atom and reads

$$\begin{aligned} H = & \sum_{i\sigma\vec{R}} E_{i,a} a^{\dagger}_{i\sigma\vec{R}} a_{i\sigma\vec{R}} + \sum_{i\sigma\vec{R}} E_{i,c} c^{\dagger}_{i\sigma,\vec{R}+\vec{d}} c_{i\sigma,\vec{R}+\vec{d}} \\ & + \sum_{\vec{R},\vec{R}',\sigma ij} V_{i,j} a^{\dagger}_{i\sigma\vec{R}} c_{i\sigma,\vec{R}+\vec{d}} + \text{H.c.} \\ & + \sum_{ij\sigma\sigma'\vec{R}} \frac{4\lambda_a}{\hbar} \vec{L}_{a,ij} \cdot \vec{S}_{a,\sigma\sigma'} a^{\dagger}_{i\sigma\vec{R}} a_{j\sigma'\vec{R}} \\ & + \sum_{ij\sigma\sigma'\vec{R}} \frac{4\lambda_c}{\hbar} \vec{L}_{c,ij} \cdot \vec{S}_{c,\sigma\sigma'} c^{\dagger}_{i\sigma\vec{R}+\vec{d}} c_{j\sigma'\vec{R}+\vec{d}}, \end{aligned} \tag{1}$$

where $a^{\dagger}_{i\sigma\vec{R}}$ and $c^{\dagger}_{i\sigma,\vec{R}+\vec{d}}$ are the creation operators for electrons on the *anion* and *cation* sites, respectively, *i*

$=(s,s^*,p_x,p_y,p_z)$ is the orbital index, and σ is the spin index. $E_{i,a}$, $E_{i,b}$, and $V_{i,j}$ are the tight-binding parameters defined by Slater and Koster.[14] Spin-orbit coupling is contained in the last two terms and is represented by two coupling constants λ_a and λ_b. The tight-binding parameters are taken from Ref. 15 where they were determined by fitting to a first-principles calculation.

To obtain the boundary (edge or surface) states for quasi-2D HgTe/CdTe quantum well structures and for the bulk 3D materials, we apply the Green's function method[16,17] based on the TB model described above. For the quantum well system, we consider a symmetric HgTe/CdTe heterostructure with a fixed $N_c=8$ layers of CdTe surrounding a variable N_h layers of HgTe on each side. In order to calculate the boundary states, we choose open boundary conditions along the x direction, periodic boundary conditions along the y direction, and open boundary conditions along the z direction which is the growth direction of the quantum well. For the bulk materials, surface states can be calculated for a semi-infinite system with open boundary conditions on one direction, such as [001], and periodic boundary conditions on the other two directions. The inverse Green's functions of both the quantum well and bulk materials can be written in a block tridiagonal form as

$$G^{-1}(z) = z - H = \begin{pmatrix} z-H_0 & C & 0 & 0 \\ C^\dagger & z-H_0 & C & 0 \\ 0 & C^\dagger & z-H_0 & C \\ 0 & 0 & C^\dagger & \cdots \end{pmatrix},$$

where the diagonal block H_0 describes the Hamiltonian within the same "principal layer,"[16] that is, the layer whose plane is perpendicular to the x axis (the x direction has open boundary conditions) for the quantum well case or that with plane layers perpendicular to the direction with open boundary conditions for the bulk case. The off-diagonal block C describes the coupling between two nearest-neighbor principal layers. To study the boundary states, we only need g_{ij}, the Green's function on the boundary, where i,j are the indices of the local basis on the boundary. This function is contained in the first diagonal block of the matrix $G(z)=(z-H)^{-1}$ and can be expressed in a recursive way as $g_{ij}^{(N)}=(z-H_0-Cg^{(N-1)}C^\dagger)_{ij}^{-1}$ with $g_{ij}^{(N)}$ denoting the boundary Green's function for a system with N principal layers. The above recursive equations can be closed by the initial condition $g_{ij}^{(1)}=(z-H_0)^{-1}$, and we obtain $g_{ij}^{(N)}$ iteratively. Any physical observables projected onto the boundary are easily expressed using these Green's functions as $-\frac{1}{\pi}\int d\omega \Sigma_{ij} \mathrm{Im}\, g_{ij}^{(N)}(\omega+i0^+)O_{ji}=-\frac{1}{\pi}\int d\omega \rho_o(\omega)$, where $\rho_o(\omega)$ is a type density of states and i,j run over all the local basis states on the boundary. For example, $O^c=\Sigma_i|i\rangle\langle i|$ and $O^s=\Sigma_{ij}L_{ij}^z+S_{ij}^z$ generate the density of states for charge and spin on the boundary respectively. Notice here that we generalize the definition of "spin" to include all the local angular momenta with real spin and angular momentum of the local basis. This method is easily generalized to study the interface states between two semi-infinite crystals, e.g., HgTe and CdTe, which is essential in the present work, as will be explained below.

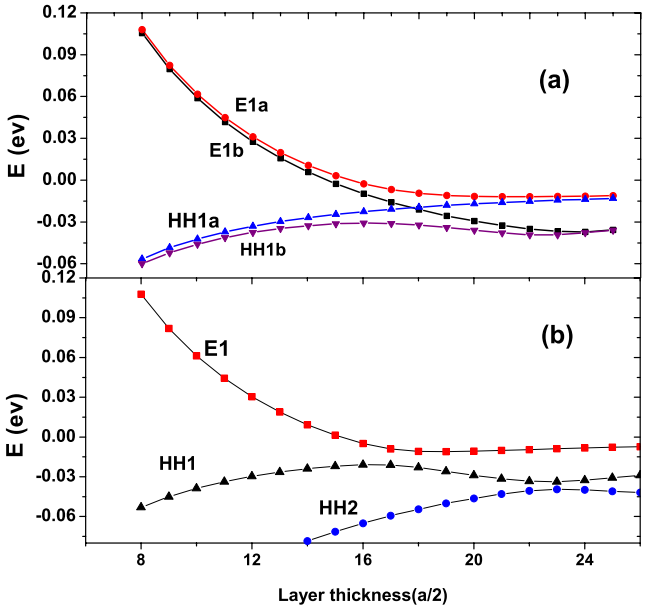

FIG. 1. (Color online) (a) The subband splitting as a function of layer thickness at one of the "crossing points" $\mathbf{k}=(0.017,0.008)\frac{\pi}{a}$. (b) The subband splitting as a function of layer thickness at the Γ point.

III. HgTe/CdTe QUANTUM WELL

As is well known for HgTe quantum wells, the confinement effect along the z direction opens a small gap around the Fermi level which makes the quantum well an insulator. By the analysis in Ref. 1 based on the $\mathbf{k}\cdot\mathbf{P}$ approximation, a quantum phase transition from a topologically trivial phase to a nontrivial phase (QSH phase) occurs for HgTe/CdTe quantum wells at some critical thickness of the HgTe layer, which is signaled by a level crossing between the E1 and HH1 subbands. We study this transition using the more realistic full TB Hamiltonian given above. First, we choose periodic boundary conditions in x and y to obtain the 2D subband spectrum for different thicknesses N_h of HgTe layers. In Fig. 1(b), we plot the subband spectrum at the Γ point as a function of HgTe "halflayers." Whereas Ref. 1 predicts that the subbands will cross, we find an anticrossing at the Γ point at a critical layer thickness $d_c=9a$. This difference between the work of Ref. 1 and these TB results can be explained by the presence of BIA in the zinc-blende lattice which is ignored in the previous paper. From the $\mathbf{k}\cdot\mathbf{P}$ perspective, an additional term $H'=C_k k_z\{J_z,(J_x^2-J_y^2)\}$ is allowed in the bulk Hamiltonian once the point-group symmetry is reduced by BIA to D_{2D},[18] with J_x,J_y,J_z the spin-3/2 matrices. Despite being a k_z-dependent term in the bulk system, in the quantum well, H' generates a constant term with *finite* matrix elements connecting the $|E1\pm\rangle$ subbands with the $|HH1\mp\rangle$ subbands near the Γ point, which can be derived following the effective 2D $\mathbf{k}\cdot\mathbf{P}$ approach of Refs. 1 and 19. This term qualitatively affects the physics in exactly the manner predicted by the TB model.

Upon further investigation, we find that the inversion asymmetry shifts the crossing point from the Γ point to eight

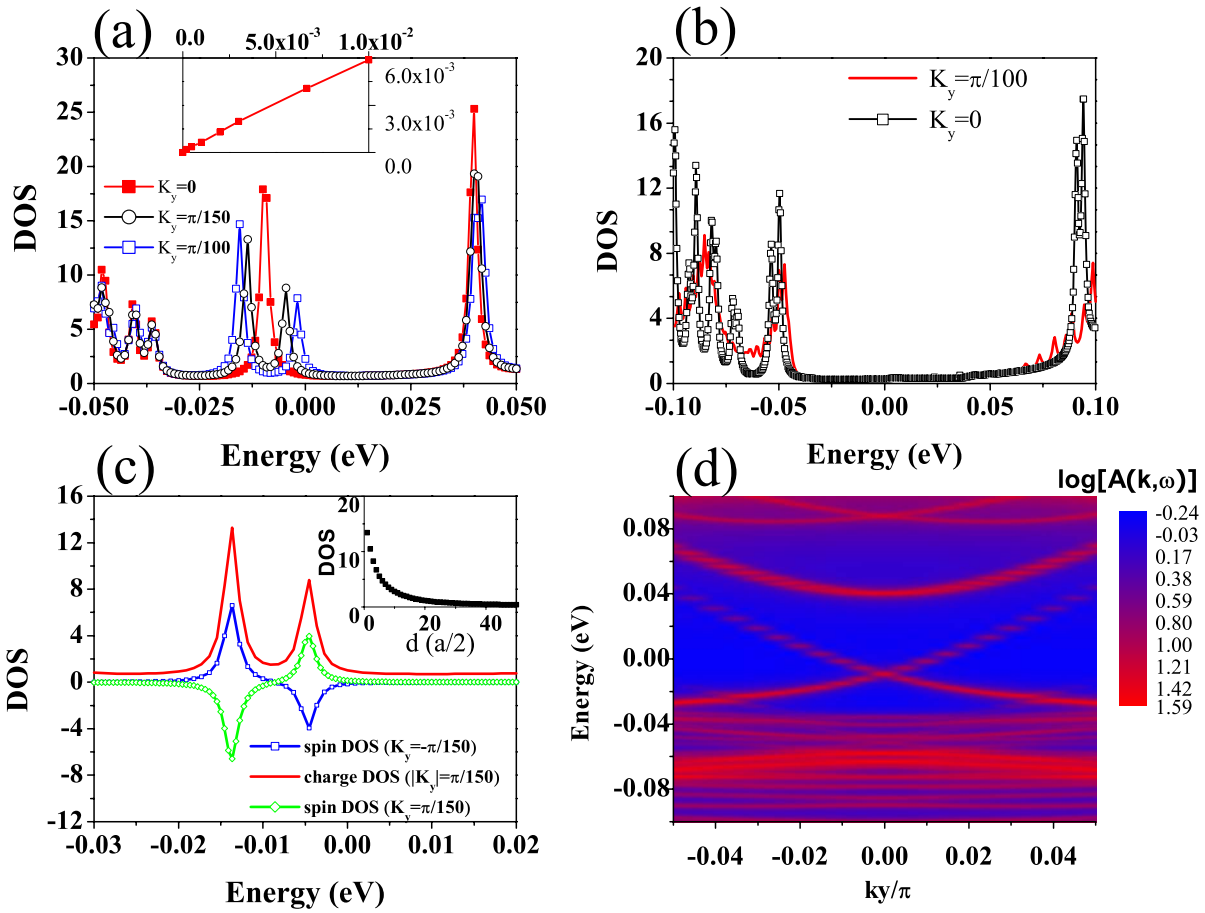

FIG. 2. (Color online) (a) The density of states at the edge of the quantum well with layer thickness $d=20(a/2)$. (The inset plot shows the linear energy splitting of the edge states in the very small region near $k_y=0$.) (b) The density of states at the edge of the quantum well with layer thickness $d=10(a/2)$. (c) The spin density of states at the edge of the quantum well with thickness $d=20(a/2)$. (The inset plot shows the decay of density of states at the peak energy of the spectra with $k_y=0$.) (d) The intensity color plot on the energy-momentum plane for the density of states at the edge of the quantum well with thickness $d=20(a/2)$. We have taken the logarithm of the intensity so that nonzero intensity clearly stands out.

nonzero k points around it. In Fig. 1(a), we plot the subband spectrum at one of these crossing points $\mathbf{k}=(0.017,0.008)\frac{\pi}{a}$ where a clear level crossing between E1 and HH1 is observed. (Notice that away from the Γ point, the inversion asymmetry removes the double degeneracy as expected.) The other seven crossing points are determined by the point-group star of this one. We find that even if the level crossing at the Γ point is avoided, the gap-closing quantum phase transition between two insulating regimes previously proposed in the simplified model still exists.

After identifying the presence of the quantum phase transition, the next natural question is whether the topologically nontrivial phase on the thicker side of the transition predicted by the $\mathbf{k}\cdot\mathbf{P}$ calculation will survive the inversion symmetry breaking. The most convincing way to answer this question is to calculate the edge states directly. By the recursion method, we obtain the charge and spin densities of states defined above. The charge density of states for a quantum well structure with 20 and 10 half-layers are plotted in Figs. 2(a) and 2(b), respectively. Sharp peaks appear in the gap for the quantum well with 20 half-layers and are absent in the 10 half-layer system. As required by the time-reversal symmetry, the energy levels at the Γ point *must* be doubly degenerate but can be split at finite k_y. The energy level splitting near $k_y=0$ as a function of k_y is plotted in the inset of Fig. 2(a), which shows a perfect linear dispersion indicating a level crossing of the edge states at $k_y=0$. The spin densities of states for two k_y's with opposite signs are plotted in Fig. 2(c). If the chemical potential lies between the two peaks, only the lower branch of the edge states is occupied and a spin current will be carried by the edge states. With the recursion method, we can also obtain the charge density of states on the internal layers away from the edge. In the inset of Fig. 2(c), we plot the height of the in-gap peak for $k_y=0$ on the different layers, which decays rapidly as you move away from the edge and thus demonstrates that the in-gap peak is produced by the edge states. Finally, we plot the edge state dispersion in Fig. 2(d) with a color intensity plot generated from the density of states. We have plotted the logarithm of the intensity so that nonzero intensity clearly stands out. We find that the edge states merge with the bulk states as k_y moves away from the Γ point. Consequently, whenever the chemical potential lies in the bulk gap, the only low-energy states crossing the

Fermi level are *a single* Kramers pair of edge states. In other words, the low-energy behavior of the quantum well in the bulk insulating region is described by an odd number of pairs of one-dimensional (1D) channels propagating on each edge. According to Ref. 7, such a 1D liquid is a "helical liquid" and cannot be realized in any pure 1D system that preserves TRS. It can only exist as the edge theory of a 2D QSH insulator. In this way, the results of our calculations provide convincing evidence that the HgTe/CdTe quantum well is a QSH insulator characterized by a nontrivial Z_2 topological invariant.[3]

IV. BULK HgTe AND HgTe/CdTe INTERFACE

The same recursion method can also be applied for the 2D surface states of strained 3D HgTe, which was recently suggested to be topologically nontrivial.[13] However, the TB model [Eq. (1)] applied to a semi-infinite system with a 2D surface always generates some surface states, even for a trivial band insulator, e.g., CdTe.[17] Physically, these surface states correspond to a dangling sp^3-hybridized bond at each surface atom and are thus strongly dependent on the details of the surface physics, such as surface reconstruction and disorder. On the other hand, as we will show below, the topology of the surface states for the trivial insulator CdTe and topological insulator HgTe are quite different, and we can still distinguish them. Since in the present paper we are only concerned about the topological properties, which are insensitive to the details of surface physics, we can choose a surface regularization that removes the trivial surface states and leaves only the topological ones. Therefore, we have also studied the interface between bulk HgTe and CdTe, where the dangling bonds of HgTe are coupled to CdTe and saturated so that the trivial surface states vanish. Since CdTe can be adiabatically connected with vacuum by taking its band gap to infinity, the topological properties of a HgTe/CdTe interface are determined by HgTe and do not depend on the choice of the surface regularization.

Since bulk HgTe is a semimetal, we need to apply a small compressive strain, along, say, the [001] direction, to make it an insulator. The tight-binding parameters for strained HgTe are obtained by fitting the local density approximation results from the plane wave pseudopotential method.[20]In the present paper, we apply the strain along the [001] direction (z direction) and put the HgTe surface along both the [100] (x direction) and [001] directions. For both cases, we find nontrivial surface states.

The densities of states on the surface for both strained HgTe and CdTe are shown in Fig. 3 by the color intensity plot, from which we can see clearly that both of them have surface states in the gap. Again, we have plotted the logarithm of the intensity so that nonzero intensity clearly stands out. The existence of the surface state in CdTe and HgTe has been known for a few decades,[21–23] while their topological structure has never been studied carefully. Although the surface states in HgTe and CdTe look quite similar, there is an essential topological difference between them. The surface states for CdTe have level crossings at all the high symmetry points: (0, 0), (π,π), $(2\pi,0)$, $(0,2\pi)$. In contrast, the HgTe

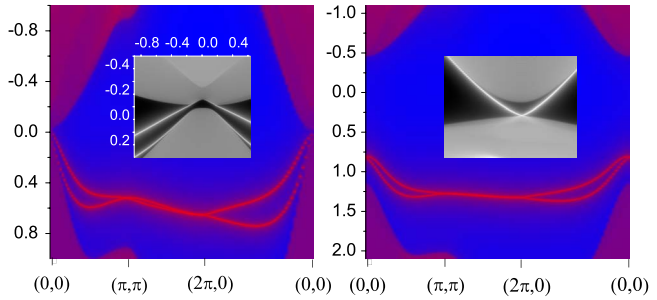

FIG. 3. (Color online) Intensity color plot in the energy-momentum plane for the density of states at the HgTe (left) and CdTe (right) (100) surfaces. The uniaxial strain is applied along the [001] direction for HgTe by choosing the c/a ratio to be 0.98. We have taken the logarithm of the intensity so that nonzero intensities clearly stand out.

surface states merge into the bulk bands near the Γ point (as shown in the inset of Fig. 3) but behave similar to CdTe in the rest of the BZ. We also plot the Fermi surface of the surface states for both HgTe and CdTe in Fig. 4. We find that for HgTe, if the Fermi energy remains inside the bulk gap, only one Fermi surface crossing will be detected when sweeping from the Γ point to the zone boundary. On the other hand, for CdTe, you will either find zero or an even number of Fermi surface crossings. This even and/or odd difference between CdTe and HgTe reflects the different Z_2 classifications and can be detected directly by angle resolved photoemission spectroscopy (ARPES).

In Fig. 5, we plot the density of states on the HgTe/CdTe interface in a color intensity plot where we have plotted the logarithm of the intensity so that nonzero intensity clearly stands out. As we discussed before, the trivial surface states of HgTe with CdTe added to the surface are removed by saturating the dangling bonds. The single pair of surface states is clearly seen in the bulk insulating gap and they cross at the Γ point. There are no other surface states in the entire zone. Any pure 2D band theory that respects TRS must have the same number of Kramer pairs on each of the time-reversal symmetric wave vectors because all of the $2N$ energy bands must be paired on these wave vectors. As a result, the 2D surface states of HgTe cannot emerge from any

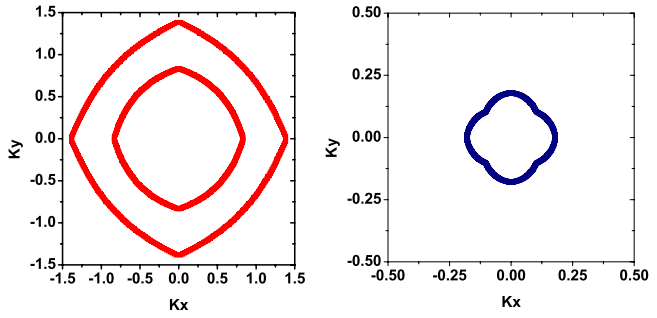

FIG. 4. (Color online) The shape of the Fermi surface at the (100) surface of CdTe (left) and HgTe (right). The uniaxial strain is applied along the [001] direction for HgTe by choosing the c/a ratio to be 0.98.

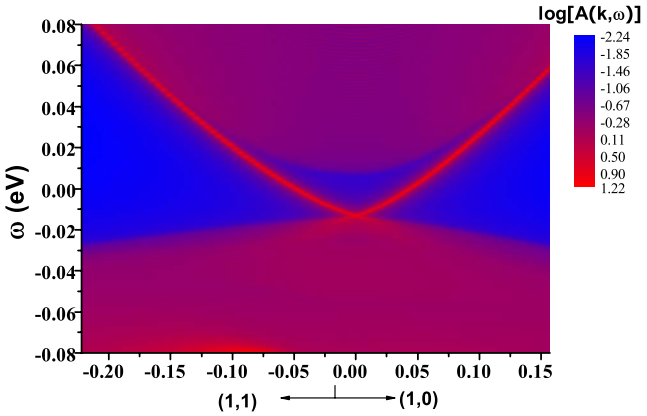

FIG. 5. (Color online) Intensity color plot in the energy-momentum plane for the density of states at the HgTe/CdTe interface. The uniaxial strain is applied along the [001] direction by choosing the c/a ratio to be 0.98, and the HgTe/CdTe interface is chosen along the [100] direction. We have taken the logarithm of the intensity so that nonzero intensity clearly stands out.

pure 2D surface effect and only as a consequence of bulk topology.

It is useful to try to understand this result from a continuum $\mathbf{k}\cdot\mathbf{P}$ perspective. HgTe has a nontrivial topological structure because the band structure is only "inverted" near the Γ point. The fact that an occupied band at this point has Γ^6 character means that the Z_2 invariant picks up an extra factor of -1 (if we ignore the small BIA) when compared to CdTe (or vacuum), making it nontrivial. Due to the strong orbital mixing, the Γ^6 character is washed out as one moves away from the Γ point, and at the other special TR invariant points, the inverted structure is absent. Therefore, we should be able to understand the topological properties from the band structure only near the Γ point. The key point is to consider the six-band Kane model[24] instead of just the reduced four-band Luttinger model. If we only keep the bands in the Luttinger model, the topological structure is absent because the inclusion of the Γ^6 band is essential. In the presence of uniaxial compressive strain along the (001) direction, an insulating gap opens between the heavy-hole (HH) and light-hole (LH) bands by pushing the HH band downward in energy. For a moment, we will ignore the HH band and focus only on the LH and Γ^6 (E) band. From the form of the Kane model, the coupling of the LH and E bands near the Γ point is exactly a 3D anisotropic massive Dirac Hamiltonian (if we ignore BIA and keep the leading order in k). The Dirac Hamiltonian preserves parity symmetry and we can label the bands by parity eigenvalues. Since the coupling is linear, there must be one even (doubly degenerate) and one odd (doubly degenerate) band. We expect that when the odd parity band lies below the even band, then there will be a nontrivial Z_2 invariant which indicates an odd number of pairs of surface states that cross at TR invariant points.[13] The presence of the HH band will change the features of the spectrum but it does not change the presence of the surface states, or their protected crossing, as long as the strain gap is open. The system will remain a 3D topological insulator when the HH band is coupled and when BIA terms are added, as long as the bulk gap does not close. To show evidence of our statements, we solve the six-band Kane model on a cylinder. First, we solve the model with the HH band *completely* decoupled from the LH and E bands [Fig. 6(a)]. Here, the HH band remains flat and is split from the LH band by the strain gap. In the gap, there are clear, linearly dispersing surface states which traverse the gap between the LH and E bands. Nothing occurs at the other special points in the BZ so this is a strong topological insulator. Turning on the coupling to the HH band changes features of the band structure but does not change the topology of the state since the gap between the LH and HH bands never closes. It is clear from Fig. 6(b) that even when the HH band is fully coupled, the system is still a strong topological insulator with surface states crossing at Γ.

More rigorously, the nontrivial bulk topology leading to the surface states is characterized by four Z_2 invariants.[5,6,13] According to Ref. 13, the Z_2 invariants can be understood in terms of "time-reversal polarization," $\pi_a = \pm 1$, which is defined for the four TR symmetric momenta Λ_a, $a=1,2,3,4$, in a certain 2D projection of the BZ. Along a path from Λ_a to Λ_b, the surface state Kramer pairs will switch partners if and only if $\pi_a \pi_b = -1$, as shown in Figs. 7(a) and 7(b). From the surface state dispersion of HgTe shown in Fig. 3, one can see that a pair of surface states at the Γ point splits and merges separately into bulk bands at finite momentum, which means that they become Kramers partners of other states at the other

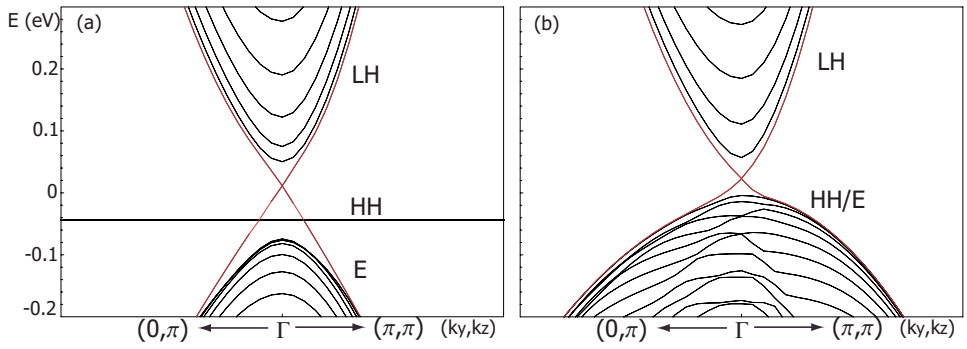

FIG. 6. (Color online) Band structure near the Γ point for (a) decoupled HH band and (b) full HH band coupling. Surface sates are located in the bulk gap in both subfigures and are shown in red. Gap due to strain is artificially large so that surface states are clearly visible. However, the states will exist for any finite compressive strain.

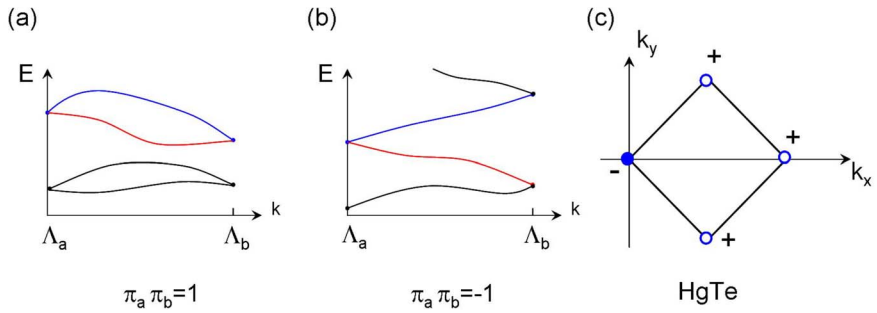

FIG. 7. (Color online) [(a) and (b)] Schematic picture of the energy band dispersion along a path between two symmetric points Λ_a, Λ_b for (a) $\pi_a\pi_b=1$ and (b) $\pi_a\pi_b=-1$. (c) The time-reversal polarization of HgTe surface states.

three TR invariant momenta $(\pi,0)$, $(0,\pi)$, (π,π). In other words, the "partner switch" happens between (0, 0) and all the other three TR symmetric points, which means $-\pi_{(0,0)}=\pi_{(\pi,\pi)}=\pi_{(\pi,-\pi)}=\pi_{(2\pi,0)}$, as shown in Fig. 7(c). Consequently, our calculation shows that the uniaxial strained bulk HgTe is a strong topological insulator under the definition of Refs. 5 and 13. This is in agreement with the statement of Ref. 13 based on an adiabatic continuity argument between strained HgTe and α-Sn.

In conclusion, this work has supplied numerous realistic numerical results that support the earlier work done on topological insulators with simplified models. We showed that for the 2D QSH effect, the BIA terms are not strong enough to destroy the QSH phase (by closing the bulk gap) and the quantum phase transition still occurs as a function of quantum well thickness. Using realistic tight-binding models and first-principles calculations, we have clearly shown that CdTe is a trivial topological insulator and compressively strained HgTe is a nontrivial topological insulator. We showed this by calculating the band structure of each material with unsaturated surface bonds which shows both trivial and nontrivial surface states. Additionally, we showed that for strained HgTe with its dangling surface bonds saturated by CdTe that the topologically protected surface states exist only around the Γ point, just as our analytic arguments predict. Finally, we gave examples of Fermi surface cuts that would be measurable by ARPES experiments and gave arguments about the Z_2 index in these materials.

ACKNOWLEDGMENTS

This work is supported by the NSF under Grant No. DMR-0342832 and the U.S. Department of Energy, Office of Basic Energy Sciences, under Contract No. DE-AC03-76SF00515, the Focus Center Research Program (FCRP) Center on Functional Engineered Nanoarchitectonics (FENA), and the Knowledge Innovation Project of the Chinese Academy of Sciences.

[1] B. A. Bernevig, T. L. Hughes, and S. C. Zhang, Science **314**, 1757 (2006).
[2] M. Konig, S. Wiedmann, C. Brune, A. Roth, H. Buhmann, L. Molenkamp, X.-L. Qi, and S.-C. Zhang, Science **318**, 766 (2007).
[3] C. L. Kane and E. J. Mele, Phys. Rev. Lett. **95**, 146802 (2005).
[4] B. A. Bernevig and S. C. Zhang, Phys. Rev. Lett. **96**, 106802 (2006).
[5] L. Fu, C. L. Kane, and E. J. Mele, Phys. Rev. Lett. **98**, 106803 (2007).
[6] J. E. Moore and L. Balents, Phys. Rev. B **75**, 121306(R) (2007).
[7] C. Wu, B. A. Bernevig, and S. C. Zhang, Phys. Rev. Lett. **96**, 106401 (2006).
[8] C. Xu and J. E. Moore, Phys. Rev. B **73**, 045322 (2006).
[9] S. Murakami, N. Nagaosa, and S. C. Zhang, Science **301**, 1348 (2003).
[10] J. Sinova, D. Culcer, Q. Niu, N. A. Sinitsyn, T. Jungwirth, and A. H. MacDonald, Phys. Rev. Lett. **92**, 126603 (2004).
[11] S. Murakami, N. Nagaosa, and S. C. Zhang, Phys. Rev. B **69**, 235206 (2004).
[12] S. Murakami, N. Nagaosa, and S. C. Zhang, Phys. Rev. Lett. **93**, 156804 (2004).
[13] L. Fu and C. L. Kane, Phys. Rev. B **76**, 045302 (2007).
[14] J. Slater and G. Koster, Phys. Rev. **94**, 1498 (1954).
[15] A. Kobayashi, O. F. Sankey, and J. D. Dow, Phys. Rev. B **25**, 6367 (1982).
[16] I. Turek, V. Drchal, J. Kudrnovsky, M. Sob, and P. Weinberger, *Electronic Structure of Disordered Alloys, Surfaces and Interfaces* (Kluwer Academic, Boston, 1997).
[17] G. W. Bryant, Phys. Rev. B **35**, 5547 (1987).
[18] R. Winkler, *Spin-Orbit Coupling Effects in Two-Dimensional Electron and Hole Systems*, Springer Tracts in Modern Physics (Springer, New York, 2003).
[19] T. L. Hughes, C.-X. Liu, X.-L. Qi, and S.-C. Zhang (unpublished).
[20] Z. Fang and K. Terakura, J. Phys.: Condens. Matter **14**, 3001 (2002).
[21] M. Dyakonov and A. Khaetskii, JETP Lett. **33**, 110 (1981).
[22] Y. R. Lin-Liu and L. J. Sham, Phys. Rev. B **32**, 5561 (1985).
[23] O. A. Pankratov, S. V. Pakhomov, and B. A. Volkov, Solid State Commun. **61**, 93 (1987).
[24] E. O. Kane, J. Phys. Chem. Solids **1**, 249 (1957).